Rock and Soil Mechanics

Volume 41 | Issue 2 Article 2

9-27-2020

Stability analysis of slope based on Green-Ampt model under heavy rainfall

Yong-hua SU

Cheng-cheng LI
Lcc_ah@163.com

Custom Citation

SU Yong-hua, LI Cheng-cheng. Stability analysis of slope based on Green-Ampt model under heavy rainfall[J]. Rock and Soil Mechanics, 2020, 41(2): 389-398.

Rock and Soil Mechanics 2020 41(2): 389−398 ISSN 1000−7598
https: //doi.org/10.16285/j.rsm.2019.5001 rocksoilmech.researchcommons.org/journal

Stability analysis of slope based on Green-Ampt model under heavy rainfall

SU Yong-hua, LI Cheng-cheng
College of Civil Engineering, Hunan University, Changsha, Hunan 410082, China

Abstract: The method of rainfall infiltration analysis directly affects the prediction and prevention of rainfall-induced landslides. Green-Ampt (GA) model, which has clear physical meaning and few parameters, has been paid more and more attention in the analysis of rainfall-induced landslides. However, this method ignores the existence of the unsaturated layer of the wetting layer and the seepage of the saturated layer, which affects the calculation accuracy. In view of the above deficiencies, the LSGA model is established based on the stratified hypothesis and the saturated layer seepage, and the expression of slope stability coefficient is established. All results show that LSGA model can be simplified to GA model for infinite slope without considering the stratified hypothesis of wetting layer, which indicates that GA model is a special case of LSGA model. The slope infiltration depth and instability time of GA are obviously behind the LSGA model. The saturated layer seepage has slight effect on the characteristics of the wetting layer, but has a great influence on the stability of slope. On the contrary, the effect of slope length on wetting layer characteristics is important, but the effect on slope stability is slight. All results obtained by using LSGA model and the stability evaluation method are basically consistent with the phenomena revealed by the model test, which proves that the method has better accuracy and reliability than others.

Keywords: rainfall infiltration; Green-Ampt model; stratified hypothesis; seepage; slope stability

1 Introduction

Landslide has been becoming one of the most dangerous geo-hazards due to its high frequency, large scale and severe damage[1]. It has been reported that there are about 1.5×10^4 landslides in China, and the related economic loss is up to tens of billions Yuan every year[2]. Therefore, the research on the control of landslides is of great importance nowadays. Rainstorms with long term and great intensity have been the most common causes of slope instability [3–4]. Rainwater infiltrates into soils and increases water content, leading to the decrease of the shear resistance of soils. Meanwhile, the unit weight of soils increases, leading to the increase of the sliding force of the slope. In addition, the seepage forces induced by the infiltration of the rainwater would increase the sliding force of the slope as well.

The method of rainfall infiltration accompanied with the stability analysis is an effective way to analyze the slope stability under rainfall. Green-Ampt (GA) model[5], which has clear physical meaning and few parameters, has been paid more and more attention in the analysis of rainfall-induced landslides [6–7]. Cho[8] applied a shallow and impermeable boundary condition in the GA model, and combined it with the limit equilibrium method to study the stability of a residual soil slope which has an impervious bedrock as potential sliding surface under different rainfall intensities. Wang et al.[9] discussed the seepage in the saturated layer parallel to the slope surface and the induced seepage force. However, the variation of water content in the unsaturated layer was not considered. Tang et al.[10] studied the influence of the initial water content on slope stability using the enhanced GA model, in which the unsaturated flow was considered by the VG model. Loáiciga et al.[11] formulated an infiltration-runoff model by combining the GA model with the governing run-off equation, and discussed the slope stability with the model.

The previous studies have greatly extended the scope of application of the GA model. However the unsaturated layer was not considered. Wang et al.[12] and Peng et al.[13] reported that the water content in the unsaturated layer varies with the depth. Based on Peng et al.[13], Zhang et al.[14] proposed a method for the stability analysis for the stratified slope. However, it is mainly applicable to the situation of collected water on the slope, and the effect of rainfall intensity could not be considered directly. Yao et al.[15] assumed that the depth of wetting front is evenly split between saturated layer and unsaturated layer. However, the influence of the stratification of slope on the infiltration rate was not considered. Moreover, the seepage in the saturated layer parallel to the slope surface and the induced seepage force were not considered.

In view of the above deficiencies, the present study attempts to propose a model (LSGA model) for rainfall infiltration

Received: 2 January 2019 Revised: 29 May 2019
This work was supported by the National Natural Science Foundation of China (51578232, 51878266).
First author: SU Yong-hua, male, born in 1965, PhD, Professor, PhD supervisor，Research interests: reliability of geotechnical engineering. E-mail: yong_su1965@126.com
Corresponding author：LI Cheng-cheng, male, born in 1991, Master degree candidate, majoring in geotechnical engineering. E-mail: Lcc_ah@163.com

analysis on the basis of the previous works [13]. It is able to consider the variation of water content in the unsaturated layer and the seepage in the saturated layer parallel to the slope surface. The LSGA model was then applied to analyze the stability of a slope under rainfall.

2 LSGA model

According to the infiltration test results and the simulation results by Richards equation, Peng et al.[13] divided the soils under infiltration surface into the saturated layer, the transition layer and the initial layer. They found that the changes of water content from the transition layer to the initial layer coincide with elliptical distribution. Thus, they proposed the stratified hypothesis as shown in Fig.1. The water contents of soil layers of different depths are given as follows [15]:

in saturated layer:

$$\theta(h)=\theta_s,\ 0\leqslant h\leqslant h_s \tag{1}$$

in transitional layer:

$$\theta(h)=\theta_d+(\theta_s-\theta_d)\sqrt{1-[(h-h_s)/h_w]^2},\ h_s\leqslant h\leqslant h_d \tag{2}$$

in initial layer:

$$\theta(h)=\theta_d,\ h\geqslant h_d \tag{3}$$

in which

$$h_s=h_d-h_w=(1-\lambda)h_d \tag{4}$$

where h_s and h_d are the depths of saturated layer and wetting layer, respectively in the direction normal to slope surface; θ_s and θ_d are the saturated water content and initial water content; h_w is the thickness of transition layer; λ is the proportion of transitional layer in the wetting layer.

With continuous rainfall, the wetting layer develops downward, but the proportion of transitional layer in the wetting layer decreases linearly [13]:

$$\lambda=ah_d+b \tag{5}$$

where a and b are model constants with $a<0$ and $0<b<1$.

From Eq. (5), there is a moment t'_p such that $\lambda=0$.

When $\lambda>0$,

$$h_d=\frac{(1-b)-\sqrt{(1-b)^2-4ah_s}}{2a} \tag{6}$$

$$h_w=\frac{(1-b)-\sqrt{(1-b)^2-4ah_s}}{2a}-h_s \tag{7}$$

The accumulated rainwater infiltration could be calculated by:

$$I=\int_0^h[\theta(h)-\theta_d]\mathrm{d}h \tag{8}$$

Since the wetting layer consists of the saturated layer and the transitional layer, the accumulated infiltration could be calculated separately:

Water content in the saturated layer is

$$I_s=(\theta_s-\theta_d)h_s \tag{9}$$

Water content in the transitional layer is

$$I_w=\frac{\pi}{4}(\theta_s-\theta_d)h_w \tag{10}$$

Then

$$I=I_s+I_w=(\theta_s-\theta_d)h_s+\frac{\pi}{4}(\theta_s-\theta_d)h_w \tag{11}$$

Substituting Eq. (7) into Eq. (11),

$$I=Ah_s+B\sqrt{(1-b)^2-4ah_s}+C \tag{12}$$

with

$$A=\frac{(\theta_s-\theta_d)(4-\pi)}{4} \tag{13}$$

$$B=-\frac{\pi(\theta_s-\theta_d)}{8a} \tag{14}$$

$$C=\frac{\pi(1-b)(\theta_s-\theta_d)}{8a} \tag{15}$$

Mein et al.[6] applied the GA model in the rainfall infiltration analysis and suggested that the process of rainfall infiltration should be divided into rainfall intensity controlled period and infiltration controlled period. Assuming that the intensity of rainfall is q and the angle of slope is β, at the start of rainfall the soils at the slope surface are unsaturated and the infiltration is larger than the rainfall intensity, and thus all the rainwater infiltrates into the soil. In this period, the infiltration rate of rainfall in the direction normal to the slope surface is given as:

$$i=q\cos\beta \tag{16}$$

With continuous rainfall, the soils at the slope surface become saturated, leading to the decrease of the infiltration. When the infiltration is smaller than the rainfall intensity, the surface runoff of rainwater occurs. According to stratified hypothesis [12], the infiltration rate in the direction normal to the slope surface is

$$i=K_s\left(\frac{h_s\cos\beta}{h_s}+\frac{S_f}{h_s}\right) \tag{17}$$

where K_s is the hydraulic conductivity of saturated soils and S_f is the suction force of the transitional layer acting on the saturated layer.

According to the consistency condition, there is a critical time moment t_p such that

$$q\cos\beta=K_s\frac{h_s\cos\beta+S_f}{h_s} \tag{18}$$

which gives

$$h_{sp}=\frac{S_f}{\eta\cos\beta} \tag{19}$$

where h_{sp} is the depth of the saturated layer at the moment t_p, and $\eta = q / K_s - 1$.

Substituting Eq. (19) into Eq. (12), we could get

$$I_p = \frac{AS_f}{\eta\cos\beta} + B\sqrt{(1-b)^2 - \frac{4aS_f}{\eta\cos\beta}} + C \tag{20}$$

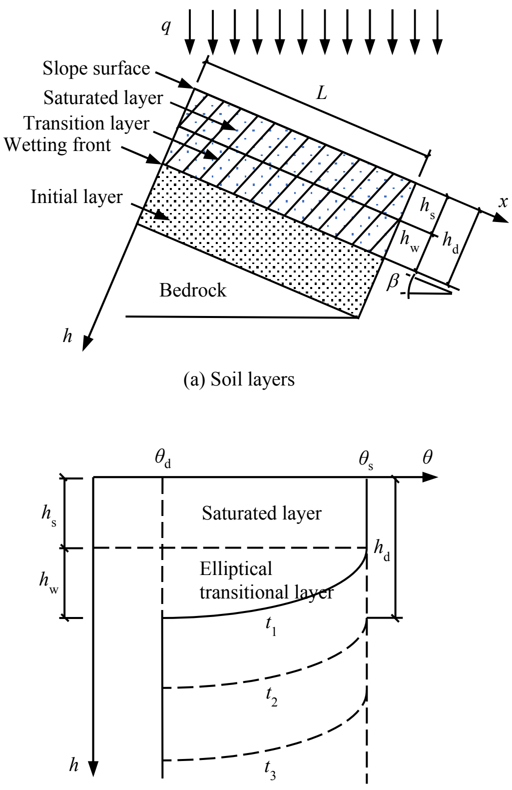

(a) Soil layers

(b) Distribution of the water content

Fig.1 Stratified hypothesis diagram

Thus, the critical time moment t_p becomes

$$t_p = \frac{I_p}{q\cos\beta} = \frac{AS_f}{q\eta\cos^2\beta} +$$

$$\frac{B}{q\cos\beta}\sqrt{(1-b)^2 - \frac{4aS_f}{\eta\cos\beta}} + \frac{C}{q\cos\beta} \tag{21}$$

Therefore, for the rainfall duration $t < t_p$, deriving t on both sides of the Eq. （12）, we could get

$$\frac{dI}{dt} = \left[A - \frac{2Ba}{\sqrt{(1-b)^2 - 4ah_s}}\right]\frac{dh_s}{dt} \tag{22}$$

Substituting Eq. (16) into Eq. （22）,

$$\frac{dh_s}{dt} = \frac{q\cos\beta}{A - \dfrac{2Ba}{\sqrt{(1-b)^2 - 4ah_s}}} \tag{23}$$

Similarly, when $t_p \leqslant t < t'_p$, for the slope of length L, Eq. （22） could be written as

$$\frac{dI}{dt} = \left[LA - \frac{2LBa}{\sqrt{(1-b)^2 - 4ah_s}}\right]\frac{dh_s}{dt} \tag{24}$$

And the rainfall infiltration rate of the stratified model is

$$\left(\frac{dI}{dt}\right)_1 = LK_s\frac{h_s\cos\beta + S_f}{h_s} \tag{25}$$

As the processing of infiltration, the wetting front keeps moving forward, and the suction force of the transition layer acting on the saturated layer decreases. Additionally, due to the gravity and the geometry condition of the slope, a part of the rainwater in the saturated layer would flow down to the bottom of the slope following the seepage paths within the slope. It is assumed that the flow paths are parallel to the slope surface. For an isotropic slope, according to the Darcy's law, the drainage rate of the saturated layer is

$$\left(\frac{dI}{dt}\right)_2 = K_s h_s\sin\beta \tag{26}$$

The effective rainfall infiltration rate is given as the difference between Eq. （25） and Eq. （26）.

$$\frac{dI}{dt} = K_s\left[\frac{L(h_s\cos\beta + S_f)}{h_s} - h_s\sin\beta\right] \tag{27}$$

By combining Eq. （24） and Eq. （27）, we could get the rate of the depth of saturated layer

$$\frac{dh_s}{dt} = \frac{K_s[L(h_s\cos\beta + S_f) - h_s^2\sin\beta]}{\left[A - \dfrac{2Ba}{\sqrt{(1-b)^2 - 4ah_s}}\right]Lh_s} \tag{28}$$

Considering the initial condition $t = t_p$ and $h_s = h_{sp}$, Eq. (28) gives the time variation of the depth of saturated layer for time $t \in [t_p,\ t'_p]$.

For $t \geqslant t'_p$, $\lambda = 0$, $h_s = h_d$, Eq. (11) could be written as

$$I = I_s = L(\theta_s - \theta_d)h_s \tag{29}$$

By deriving t on both sides of Eq. （29）, and combining it with Eq. (27) we could get

$$\frac{dh_s}{dt} = \frac{K_s[L(h_s\cos\beta + S_f) - h_s^2\sin\beta]}{(\theta_s - \theta_d)Lh_s} \tag{30}$$

In conclusion, the relationship between the variation rate of depth of saturated layer and the rainfall duration could be calculated as follows:

$$\frac{dh_s}{dt} = \begin{cases} \dfrac{q\cos\beta}{A - \dfrac{2Ba}{\sqrt{(1-b)^2 - 4ah_s}}},\ t < t_p \\ \dfrac{K_s[L(h_s\cos\beta + S_f) - h_s^2\sin\beta]}{\left[A - \dfrac{2Ba}{\sqrt{(1-b)^2 - 4ah_s}}\right]Lh_s},\ t_p \leqslant t < t'_p \\ \dfrac{K_s[L(h_s\cos\beta + S_f) - h_s^2\sin\beta]}{(\theta_s - \theta_d)Lh_s},\ t \geqslant t'_p \end{cases} \tag{31}$$

The variation rate of depth of wetting layer can then be calculated accordingly.

3 Slope stability analysis

Under rainfall infiltration, the unsaturated slopes have a relatively high risk of shallow landslides parallel to the slope surface, where the failure always occurs at the location of the wetting front. However, with the stratified hypothesis, the shear strength of the saturated layer is lower than that of wetting front, since the suction force of substrate disappears. Therefore, the interface between the saturated layer and the transitional layer (hereinafter referred to as "interface") may also become the potential sliding surface. Taking a slope with unit width and length of L as an example, we attempt to study the slope stability by using the limit equilibrium method. The seepage is assumed to be parallel to the slope surface. The wetting front surface and the interface are assumed to be the sliding surface, respectively. The diagrams for the calculation are shown in Fig. 2.

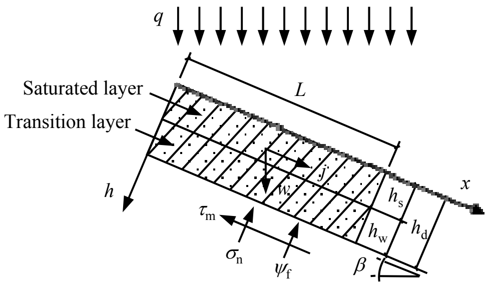

(a) When the wetting front is assumed to be the potential sliding surface

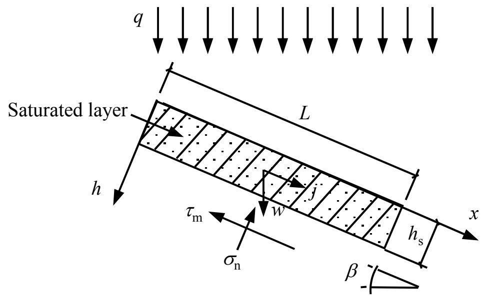

(b) When the interface is assumed to be the potential sliding surface

Fig.2 Calculating diagram of the slope

The stability of slope is evaluated by the stability coefficient F_s. It is defined as the ratio of the anti-sliding force to the sliding force of a sliding layer in unit width. When the wetting front is assumed to be the potential sliding surface, the anti-sliding forces is calculated by the Fredlund's formula for unsaturated soils[16]. When the interface is assumed to be the potential sliding surface, the anti-sliding force is calculated by the MC formula for saturated soils. For both cases, the sliding forces are the sum of the soil weight and seepage force in the direction parallel to the slope surface:

$$F_{sf} = \frac{c' + (\sigma_n - u_a)\tan\varphi' + (u_a - u_w)\tan\varphi^b}{\tau_g + j} \quad (32)$$

$$F_{sm} = \frac{c_0' + \sigma_{n0}\tan\varphi_0'}{\tau_{g0} + j} \quad (33)$$

where F_{sf} and F_{sm} are slope stability coefficients for the two cases; σ_n and σ_{n0} are the normal stresses of unsaturated and saturated soils, respectively; c', φ', c_0' and φ_0' are the effective cohesion and effective friction angle of unsaturated and saturated soils, respectively; u_a and u_w are the effective pore air pressure and effective pore water pressure; $\tan\varphi^b$ describes the effect of the substrate suction force on the shear strength of soil; τ_g and τ_{g0} are the soil unit weight of wetting layer and saturated layer, respectively in the direction parallel to the slope surface; j is the seepage force acting on the saturated layer.

Assuming that there is a linear relationship between the unit weight of soil in the transitional layer and water content, the unit weight of soil in the transitional layer could be described as

$$\gamma_h = \gamma_d + (\gamma_s - \gamma_d)\sqrt{1 - \frac{(h - h_s)^2}{h_w^2}},\ h_s \leqslant h \leqslant h_d \quad (34)$$

where γ_s is the unit weight of saturated soil, and γ_d is the initial unit weight of soil.

For $t < t_p'$:

$$\sigma_n = (\gamma_s h_s + \int_{h_s}^{h_d} \gamma_h \mathrm{d}h)\cos\beta =$$

$$\left[\gamma_s(h_s - \frac{\pi}{4}h_w) + \frac{4+\pi}{4}\gamma_d h_w\right]\cos\beta \quad (35)$$

$$\tau_g = (\gamma_s h_s + \int_{h_s}^{h_d} \gamma_h \mathrm{d}h)\sin\beta =$$

$$\left[\gamma_s(h_s - \frac{\pi}{4}h_w) + \frac{4+\pi}{4}\gamma_d h_w\right]\sin\beta \quad (36)$$

$$u_w = -\gamma_w S_f \quad (37)$$

The seepage force induced by the seepage flow parallel to the slope surface is

$$j = \gamma_w h_s \sin\beta \quad (38)$$

where γ_w is the unit weight of water.

For $t \geqslant t_p'$, let $h_w = 0$ in Eq. (35) and Eq. (36), then

$$\sigma_n = \gamma_s h_s \cos\beta \quad (39)$$

$$\tau_g = \gamma_s h_s \sin\beta \quad (40)$$

Therefore, when the wetting front is considered to be the potential sliding surface, the stability coefficient can be calculated as

$$F_{\mathrm{Sf}}=\begin{cases}\dfrac{c'+\left\{\left[\gamma_{\mathrm{s}}(h_{\mathrm{s}}-\frac{\pi}{4}h_{\mathrm{w}})+\frac{4+\pi}{4}\gamma_{\mathrm{d}}h_{\mathrm{w}}\right]\cos\beta-u_{\mathrm{a}}\right\}\tan\varphi'+(u_{\mathrm{a}}+\gamma_{\mathrm{w}}S_{\mathrm{f}})\tan\varphi^{\mathrm{b}}}{\left[\gamma_{\mathrm{s}}(h_{\mathrm{s}}-\frac{\pi}{4}h_{\mathrm{w}})+\frac{4+\pi}{4}\gamma_{\mathrm{d}}h_{\mathrm{w}}\right]\sin\beta}, & t<t_{\mathrm{p}}\\[2ex] \dfrac{c'+\left\{\left[\gamma_{\mathrm{s}}(h_{\mathrm{s}}-\frac{\pi}{4}h_{\mathrm{w}})+\frac{4+\pi}{4}\gamma_{\mathrm{d}}h_{\mathrm{w}}\right]\cos\beta-u_{\mathrm{a}}\right\}\tan\varphi'+(u_{\mathrm{a}}+\gamma_{\mathrm{w}}S_{\mathrm{f}})\tan\varphi^{\mathrm{b}}}{\left[\gamma_{\mathrm{s}}(h_{\mathrm{s}}-\frac{\pi}{4}h_{\mathrm{w}})+\frac{4+\pi}{4}\gamma_{\mathrm{d}}h_{\mathrm{w}}+\gamma_{\mathrm{w}}h_{\mathrm{s}}\right]\sin\beta}, & t_{\mathrm{p}}\leqslant t<t'_{\mathrm{p}}\\[2ex] \dfrac{c'+(\gamma_{\mathrm{s}}h_{\mathrm{s}}\cos\beta-u_{\mathrm{a}})\tan\varphi'+(u_{\mathrm{a}}+\gamma_{\mathrm{w}}S_{\mathrm{f}})\tan\varphi^{\mathrm{b}}}{(\gamma_{\mathrm{s}}+\gamma_{\mathrm{w}})h_{\mathrm{s}}\sin\beta}, & t\geqslant t'_{\mathrm{p}}\end{cases} \tag{41}$$

When taking interface as potential sliding surface,

$$\sigma_{\mathrm{n0}}=h_{\mathrm{s}}(\gamma_{\mathrm{s}}\cos\beta-\gamma_{\mathrm{w}}/\cos\beta) \tag{42}$$

$$\tau_{\mathrm{g0}}=\gamma_{\mathrm{s}}h_{\mathrm{s}}\sin\beta \tag{43}$$

the stability coefficient can then be calculated as

$$F_{\mathrm{sm}}=\begin{cases}\dfrac{c'_0+h_{\mathrm{s}}(\gamma_{\mathrm{s}}\cos\beta-\gamma_{\mathrm{w}}/\cos\beta)\tan\varphi'_0}{\gamma_{\mathrm{s}}h_{\mathrm{s}}\sin\beta}, & t<t_{\mathrm{p}}\\[2ex] \dfrac{c'_0+h_{\mathrm{s}}(\gamma_{\mathrm{s}}\cos\beta-\gamma_{\mathrm{w}}/\cos\beta)\tan\varphi'_0}{(\gamma_{\mathrm{s}}+\gamma_{\mathrm{w}})h_{\mathrm{s}}\sin\beta}, & t\geqslant t_{\mathrm{p}}\end{cases} \tag{44}$$

In a certain rainfall duration, F_{s} is the minimum of F_{sf} and F_{sm} :

$$F_{\mathrm{s}}=\min\{F_{\mathrm{sf}},F_{\mathrm{sm}}\} \tag{45}$$

Above all, under a certain rainfall intensity q, the time variation of the slope stability coefficient can be calculated by combining Eq. (31) and Eq. (45). This method considers not only the stratified wetting condition and the seepage in soils, but also different potential sliding surfaces.

4 Model verification and comparison

4.1 Comparison with the analytical solution of GA model

The GA model could not consider the stratified wetting conditions and seepage in soil. When $L\to\infty$, $a=0$, $b=0$, $h_{\mathrm{s}}=h_{\mathrm{d}}$, the LSGA model becomes the GA model, Eq. (31) could be written as

$$\frac{\mathrm{d}h_{\mathrm{s}}}{\mathrm{d}t}=\begin{cases}\dfrac{q\cos\beta}{\theta_{\mathrm{s}}-\theta_{\mathrm{d}}}, & t<t_{\mathrm{p}}\\[2ex] K_{\mathrm{s}}\dfrac{h_{\mathrm{s}}\cos\beta+S_{\mathrm{f}}}{(\theta_{\mathrm{s}}-\theta_{\mathrm{d}})h_{\mathrm{s}}}, & t\geqslant t_{\mathrm{p}}\end{cases} \tag{46}$$

Integrate Eq.(46), and substitute the initial condition $t=t_{\mathrm{p}}$, $h_{\mathrm{s}}=h_{\mathrm{sp}}$, Eq.(46) can be reformulated as

$$t=\begin{cases}\dfrac{(\theta_{\mathrm{s}}-\theta_{\mathrm{d}})h_{\mathrm{s}}}{q\cos\beta}, & t<t_{\mathrm{p}}\\[2ex] t_{\mathrm{p}}+\dfrac{(\theta_{\mathrm{s}}-\theta_{\mathrm{d}})(h-h_{\mathrm{sp}})}{K_{\mathrm{s}}\cos\beta}-\dfrac{(\theta_{\mathrm{s}}-\theta_{\mathrm{d}})S_{\mathrm{f}}}{K_{\mathrm{s}}\cos^2\beta}\ln\left(\dfrac{h\cos\beta+S_{\mathrm{f}}}{h_{\mathrm{sp}}\cos\beta+S_{\mathrm{f}}}\right), & t\geqslant t_{\mathrm{p}}\end{cases} \tag{47}$$

Eq.(47) is identical to the analytical solution of the evolution of infiltration depth with the rainfall duration in the previous study [9], which indicates that the GA model is a special case of the LSGA model.

4.2 Case study

Orense et al.[17] conducted numerous model tests to investigate the mechanism of rainfall-induced landslides. In this study, the test 8 of literature[17] is chosen as an example for analysis. In the test, the evolution of pore water pressure on bedrock and shearing displacement were monitored during the process of rainfall-induced landslides. The intensity of artificial rainfall was 171 mm/h, the upper layer was fine sand with a thickness of 20 cm, and the underlying layer was impermeable bedrock. The physical model, as well as monitoring points, are shown in Fig.3. The parameters of soil are summarized in Table 1.

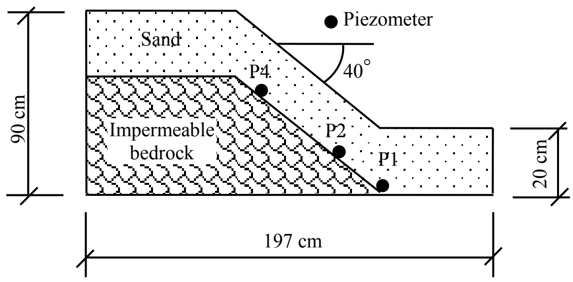

Fig.3 Testing model of slope[17]

Table 1 Soil basic parameters

γ_{d} / (kN/m^3)	γ_{s} / (kN/m^3)	K_{s} / (cm/s)	c'_0 / kPa	θ_{d}	θ_{s}	S_{f} / cm	a	b	c' / kPa	φ' / (°)	φ^{b} / (°)
16.5	21.7	1.8×10^{-4}	1.8	0.1	0.45	100	–0.027	0.91	3	36	6

Figure 4 shows the time variations of the pore water pressure, the depths of saturated layer and wetting layer. Curves P1, P2 and P4 represent the measured pore pressure. The depths of saturated layer and wetting layer are calculated using the LSGA model. It is observed that when the time t < 2 250 s, the pore water pressures change slightly. When t = 2 250 s, the pore water pressure at P4 starts to increase, which means that the wetting front has reached the depth of 20 cm. The pore water pressures of P1 and P2 increase after t = 2 397 s, which is mainly due to the fact that P1 and P2 are farther from rainfall area, leading to rainfall intensity at P1 and P2 less than 171 mm/h[17]. After the arrival of wetting front, the pore water pressures of all monitored points increase continuously until t = 3 743 s, when the saturated layer reaches the depth of 20 cm. The results confirmed the assumption that the wetting layer consists of a distinct saturated layer and a transitional layer. By using the proposed method, when t = 2 243 s, the calculated depth of the wetting layer could reach 20 cm, which fits quite well with the results of the model tests. However, when the depth of the saturated layer reaches 20 cm, the calculated time is 3 828 s, which is a little later than the results of the model tests. The main reason lies in the fact that the proposed method does not consider the effect of relatively impermeable parts in slope on the rainfall infiltration and accumulation. On the contrary, in the model test, when the wetting front reaches the monitoring points, the impermeable bedrock stops the infiltration of the rainwater, and the water accumulates on the surface of the underlying bedrock, leading to the increase of the rate of saturation.

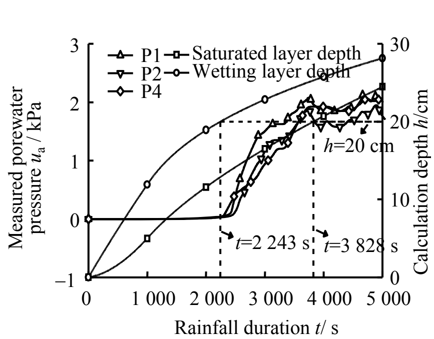

Fig.4 Time variation of measured pore pressure and calculated depths of different layers

Figure 5 shows the evolution of slope stability coefficient with rainfall duration under different conditions. The analyzed conditions are summarized in Table 2. Figure 6 shows variation of infiltration rate, wetting layer depth and saturated layer depth with rainfall duration for different models. Where i–GA is the infiltration rate calculated with GA model; h -GA is the saturated layer depth from GA model; h_d –SGA is the wetting layer depth calculated with SGA model (modified GA model only considering stratified hypothesis). Other definitions are similar with the above ones. From Fig.5 it is observed that no matter for which model, at the beginning of rainfall, the stability coefficient decreases rapidly, and in the later stage of rainfall, the stability coefficient gradually stabilizes. When t < 797 s, the SGA model and LSGA model take wetting front as potential sliding surface, while when t > 797 s, the interface becomes the potential sliding surface. The results indicated that with the process of rainfall, the position of potential sliding surface would change. Therefore, the slope stability evaluation method proposed in this paper is more comprehensive.

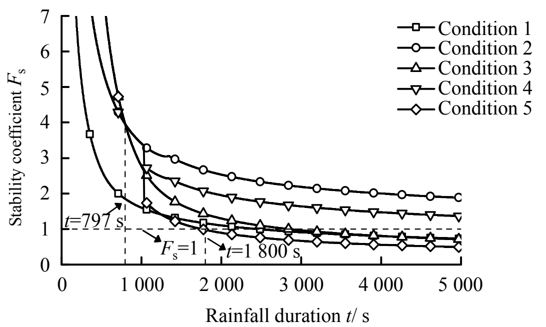

Fig.5 Variation of slope stability coefficient with rainfall duration

Table 2 Various working conditions and their calculation methods

Condition	Model	Sliding surface	Formula	Infiltration force
1	GA	Wetting front	F_{sm}	0
2	SGA	Wetting front	F_{sf}	0
3	SGA	Interface	F_{sm}	0
4	LSGA	Wetting front	F_{sf}	$\gamma_w h_s \sin\beta$
5	LSGA	Interface	F_{sm}	$\gamma_w h_s \sin\beta$

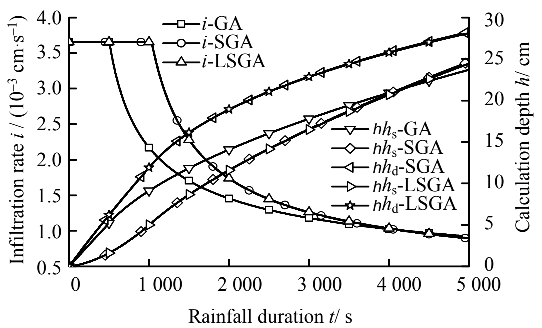

Fig.6 Variation of wetting front characteristics with rainfall duration under different working conditions

Under the same rainfall condition, according to the proposed method, the evolution of slope stability coefficient with rainfall duration could be divided into 4 stages.

Stage 1: when rainfall duration t < 797 s, SGA model = LSGA model > GA model. In this stage, the seepage flow parallel to slope surface is not considered. Thus, the calculated wetting layer depth, saturated layer depth and stability coefficient of the SAG model and LSGA model are the same, until the critical time t_p = 1 031 s. Additionally, the GA model does not consider the transitional layer, all the rainwater infiltrates into the saturated layer. Therefore, at the beginning of rainfall, the saturated layer depth of GA model would be bigger than that of SGA and LSGA models (As shown in Fig.6), but it is not much different from the depth of the wetting layer of the SGA and LAGA models. Moreover, for the GA model, the soils on the sliding surface are saturated, the shear strength would thus be lower than that of the unsaturated soils, leading to the smallest slope stability coefficient among the three models.

Stage 2: when rainfall duration 797 s < t <1 031 s, SGA model = LSGA model > GA model. In this stage, all three models take interface as the potential sliding surface in the calculation of stability coefficient, and the only variable is the depth of the saturated layer. According to Fig. 6 and the analysis in the previous stage, in this stage the saturated layer depth of the GA model is bigger than SGA and LSGA models, and its slope stability coefficient is still the smallest among the three.

Stage 3: when rainfall duration 1 031 s < t < 1 248 s, SGA model > LSGA model > GA model. In this stage, as the LSGA model takes seepage force into account, its stability coefficient decreases rapidly, but it is still higher than that of the GA model.

Stage 4: From t > 1 248 s to the moment of failure, SGA model > GA model > LSGA model. With the development of the saturated layer, the seepage force of the LSGA model acting on the saturated layer becomes much higher, which makes its stability coefficient the smallest among the three models, while the slope stability coefficient of SGA model in this stage is still higher than that of GA model. This demonstrates the importance of considering the effect of the seepage parallel to the slope surface on the evaluation of slope stability.

As shown in Fig.6 in the infiltration controlled period, since the LSGA model considers the seepage parallel to the slope surface, its increasing rate of the depth of the saturated layer is lower than that of SGA model, and its infiltration rate is higher than that of SGA model, while the difference is so small and could be ignored. Therefore, the stratified hypothesis has a significant effect on the prediction of wetting front depth and saturated layer depth, while the seepage parallel to the slope surface in saturated layer does not have significant influence on the prediction with SGA model and LSGA model.

The model test 8[17] shows that when t = 1 800 s, cracks occur at the top of slope, which implies an unstable condition of slope. At this moment, the stability coefficient of slope according to the LSGA model $F_s = 0.97 < 1$, while according to the SGA model and the GA model F_s = 1.42 and 1.16, respectively. It can be concluded that the seepage force, which is parallel to the slope surface, in the saturated layer is an important influence factor of slope stability. Thus the proposed method is more reliable. With GA model, SGA model and LSGA model, the calculated instability moment and instability depth are t = 2 451 s, 2 848 s, 1 755 s, and h = 15.85 cm, 15.85 cm, 10.19 cm, respectively. The instability moment calculated with SGA model (with stratified hypothesis) is later than that of GA model. The instability depths of SGA model and GA model are basically the same. While for LSGA model considering both stratified hypothesis and seepage in saturated layer, the instability moment is much earlier than those of GA model and SGA model, and the instability depth is smaller than those of other two models. In comparison with the LSGA model, the moment and the depth of instability for GA model and SGA model are obviously delayed.

4.3 Size effect of slope length

Along with parallel-to-surface seepage in saturated layer, slope length L was also introduced in this study, which enhanced the GA model and made it more practically useful. In order to investigate the influence of slope length on wetting layer depth and slope stability, it is assumed that there is an isotropic soil slope without underlying impermeable bedrock. The parameters are the same as those in test 8 from literature [17]. For different slope lengths, the variation of wetting layer depth with rainfall duration is shown in Fig.7, where h_d -10 denotes the wetting layer depth for LSGA model with a slope length of 10 cm. The evolution of slope stability coefficient with rainfall duration is shown in Fig.8.

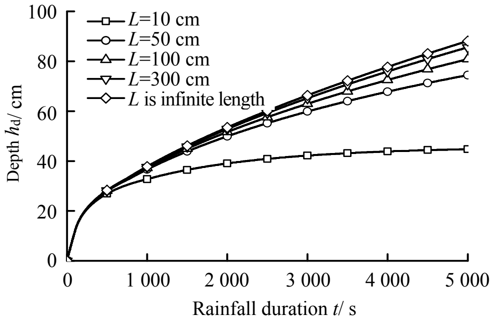

Fig.7 Variation of wetting layer characteristics with rainfall duration for different slope lengths

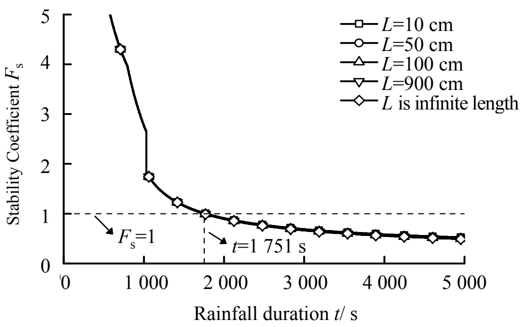

Fig.8 Variation of slope stability coefficient with rainfall duration for different slope lengths

From Fig.7, it is observed that with the increasing of rainfall duration, the wetting layer develops deeper with reducing rate. When $t<t_p$, the calculation does not consider the parallel-to-surface seepage in saturated layer. The increasing rate of wetting layer is irrelevant to the slope length. When $t\geqslant t_p$ there is a notable size effect of slope length on wetting layer. For a certain rainfall duration, the wetting layer depth increases with the slope length, while the rate of increment declines rapidly to zero. The longer the slope length is, the earlier the transitional layer disappears, and when the slope length equals to infinity, the curves obtained from the proposed model coincide with the curves from stratified model. This implies that with a short slope length, seepage in saturated layer has a greater influence on the wetting layer depth, while when the slope length approaches to infinity, the influence of the seepage flow in saturated layer could be neglected, and the model degenerates into the stratified model.

According to Fig.8, the slope stability coefficients of different slope lengths are basically the same under a certain rainfall duration. For slopes with length of 10 cm and infinity, the moments when the slope stability coefficient $F_s<1$ are 1 751 s and 1 780 s, respectively, which indicates that the size has limited effect on slope stability.

5 Discussions

In the study of Zhang et al.[14], GA model was also enhanced with stratified hypothesis, the main difference with LSGA model lies on that: their modification does not consider the parallel-to-surface seepage in saturated layer. Their enhanced GA model is mainly applicable for slopes with collected-water, the effect of rainfall intensity could not be considered directly, the infiltration rate is

$$i=K_s\left(\frac{h_0+h_s}{h_w}+\frac{S_f}{h_w}\right) \quad (48)$$

where h_0 is the thickness of collected-water on slope surface.

The infiltration rate and infiltration quantity can then be calculated according to Eq.(48). However, according to Darcy's law, this calculated infiltration rate is close to seepage flow rate in transitional layer rather than that on the slope surface, which eventually leads to a significant error. Moreover, it does not meet the infiltration rate assumption of literature [12]. This indicates that it should be the infiltration flow in the saturated layer rather than that in the transitional layer which would be influenced by the pressure potential, gravitational potential and sectional potential simultaneously. Therefore, the rainfall infiltration calculated by Eq. (17) fits better the assumption in literature [12] and the cases in practice. In the model verification of literature [14], the calculated results fit well with measured data at initial stage. However, when the wetting layer reaches 40cm, the analytical results of infiltration depth from stratified model start to be smaller than the measured results. The reasons, apart from that mentioned in literature [14], include the following two points: (i) at the initial stage, the wetting depth is small, and seepage flow rate in wetting layer is almost the same, leading to a good agreement between analytical results and measured results. With the increasing of the rainfall duration, the infiltration rate of the collected-water becomes higher than seepage rate in transitional layer; (ii) when the depth of wetting layer is higher than 40cm, the proportion of saturated layer in the wetting layer is smaller than that of transitional layer, which means the depth of saturated layer is smaller than thickness of transitional layer, leading to relatively smaller infiltration rate from Eq.(48). Additionally, according to stratified hypothesis from literature [13], at the later stage of rainfall, the proportion of transitional layer would gradually decrease to zero, during which the infiltration rate calculated from Eq.(48) would increase with approaching to infinity, which is apparently impossible.

Figure 9 shows the time variation of measured wetting front depth and the analytical results from different models. The measured data is the infiltration of collected-water from literature [13], and SGA-1 model is the infiltration model proposed by literature [16]. On the basis of SGA-1 model, SGA-2 model adopts the rainfall infiltration equation Eq.(17). It is observed that the wetting front depth calculated by Eq.(17) is larger than the measured depth, which is due to the fact that Eq.(17) considers the saturated infiltration rate, while the infiltration rate in unsaturated transitional layer is smaller than the saturated infiltration rate[15]. While compared to Eq.(48), it could predict wetting front depth more precisely.

In this study, the critical time between rainfall intensity controlled period and infiltration controlled period is an important turning point of infiltration rate. We start to consider seepage parallel to slope surface in saturated layer after the critical time, rather than from the beginning of rainfall infiltration. It is because that the soils on surface need a certain time to reach the relatively saturated condition. The stratified assumption in literature[13] does not take this period of time into consideration, leading to a drastically downward of the evolution of slope stability coefficient. Therefore, the slope stability analyses based on development of saturated layer and stratified hypothesis under heavy rainfall need to be studied further in the future.

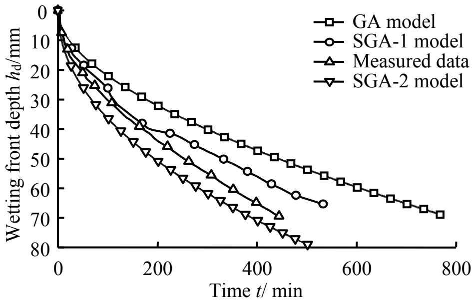

Fig.9 Wetting front depth-time curves

6 Conclusions

(1) Based on Green-Ampt soil infiltration model, the LSGA model was proposed and developed. It is able to consider the stratified wetting layer and parallel-to-surface seepage in saturated layer, and comprehensively analyze the stability of interface and wetting front. A numerical method for slope stability coefficient applicable for a whole period of rainfall infiltration was thus suggested.

(2) The comparison between different analytical results showed that GA model is a special case of LSGA model. The comparison with model tests implied a good agreement between the prediction of LSGA model and test results, demonstrating the accuracy and reliability of this method.

(3) With the increasing of rainfall duration, the coefficient of slope stability keeps decreasing. Besides, GA and SGA models have significant delays in both instability depth and time.

(4) Under the stratified hypothesis, the seepage parallel to slope surface in saturated layer is less important in the prediction of the depths of saturated layer and wetting front, while it has significant influence on the slope stability.

(5) The size effect of slope length on the wetting layer depth is obvious: wetting layer depth increases with the slope depth, while its increment rate declines rapidly to zero. However, the slope length has very slight impact on the slope stability.

References

[1] FROUDE M J, PETLEY D N. Global fatal landslide occurrence from 2004 to 2016[J]. Natural Hazards and Earth System Sciences, 2018, 18(8): 2161–2181.

[2] LIU Xin-xi, YAN E-chuan, WANG Peng-fei, et al. Nonlinear method for evaluating the landslide stability[J]. China Safety Science Journal, 2003, 13(1): 34–36.

[3] SENTHILKUMAR V, CHANDRASEKARAN S S, MAJI V B. Rainfall-induced landslides: case study of the Marappalam Landslide, Nilgiris District, Tamil Nadu, India[J]. International Journal of Geomechanics, 2018, 18(9): 05018006.

[4] PENG Jianbing, WANG Shaokai, WANG Qiyao, et al. Distribution and genetic types of loess landslides in China[J]. Journal of Asian Earth Sciences, 2019, 170: 329–350.

[5] GREEN W H, AMPT G A. Studies on soil physics[J]. Journal of Agricultural Science, 1911, 4(1): 1–24.

[6] MEIN R G, LARSON C L. Modeling infiltration during a steady rain[J]. Water Resources Research, 1973, 9(2): 384–394.

[7] DOU Hong-qiang, HAN Tong-chun, GONG Xiao-nan, et al. Reliability analysis of slope stability considering variability of soil saturated hydraulic conductivity under rainfall infiltration[J]. Rock and Soil Mechanics, 2016, 37(4): 1144–1152.

[8] CHO S E. Surficial stability analysis by the Green-Ampt infiltration model with bedrock boundary condition[J]. Journal of Korean Society of Hazard Mitigation, 2015, 15(1): 131–142.

[9] WANG Ding-jian, TANG Hui-ming, LI Chang-dong, et al. Stability analysis of colluvial landslide due to heavy rainfall[J]. Rock and Soil Mechanics, 2016, 37(2): 439–445.

[10] TANG Yang, YIN Kun-long, XIA Hui. Effects of initial water content on the rainfall infiltration and stability of shallow landslide[J]. Geological Science and Technology Information, 2017, 36(5): 204–208.

[11] LOÁICIGA H A, JOHNSON J M. Infiltration on sloping terrain and its role on runoff generation and slope stability[J]. Journal of Hydrology, 2018, 561: 584–597.

[12] WANG Wen-yan, WANG Zhi-rong, WANG Quan-jiu, et al. Improvement and evaluation of the Green-Ampt model in loess soil[J]. Journal of Hydraulic Engineering, 2003(5): 30–34.

[13] PENG Zhen-yang, HUANG Jie-sheng, WU Jing-wei, et al. Modification of Green-Ampt model based on the stratification hypothesis[J]. Advances in Water Science, 2012, 23(1): 59–65.

[14] ZHANG Jie, HAN Tong-chun, DOU Hong-qiang, et al. Analysis slope safety based on infiltration model based on stratified assumption[J]. Journal of Central South University (Science and Technology), 2014, 45(9): 3211–3218.
[15] YAO Wen-min, LI Chang-dong, ZHAN Hong-bin, et al. Time-dependent slope stability during intense rainfall with stratified soil water content[J]. Bulletin of Engineering Geology and the Environment, 2019, 78(7): 4805–4819.
[16] FREDLUND D G, MORGENSTERN N R, WIDGER R A. The shear strength of unsaturated soils[J]. Canadian Geotechnical Journal, 1978, 15(3): 313–321.
[17] ORENSE R P, SHIMOMA S, MAEDA K, et al. Instrumented model slope failure due to water seepage[J]. Journal of Natural Disaster Science, 2004, 26(1): 15–26.